SLOPE STABILITY ANALYSIS OF DHAKA CHITTAGONG HIGHWAY AT FENI SECTION CONSIDERING SOIL-WATER INTERACTION

SYED SHADMAN SAKIB
MD. SIRAJUL AREFIN
ASADUZZAMAN CHOWDHURY
FERDAUS AHMMED

ISLAMIC UNIVERSITY OF TECHNOLOGY

2017

SLOPE STABILITY ANALYSIS OF DHAKA CHITTAGONG HIGHWAY AT FENI SECTION CONSIDERING SOIL-WATER INTERACTION

SYED SHADMAN SAKIB

MD. SIRAJUL AREFIN

ASADUZZAMAN CHOWDHURY

FERDAUS AHMMED

A THESIS SUBMITTED TO THE DEPARTMENT OF CIVIL & ENVIRONMENTAL ENGINEERING OF ISLAMIC UNIVERSITY OF TECHNOLOGY (IUT) FOR THE DEGREE OF BACHELOR OF SCIENCE IN CIVIL ENGINEERING

PROJECT REPORT APPROVAL

The thesis titled “Slope stability analysis of Dhaka Chittagong highway at Feni section considering soil-water interaction” submitted by Syed Shadman Sakib, Md. Sirajul Arefin, Asaduzzaman Chowdhury and Ferdaus Ahmmed, St. No. 135412, 135447, 135416, 135448 respectively, have been found as satisfactory and accepted as partial fulfillment of the requirement for the Degree Bachelor of Science in Civil Engineering.

SUPERVISOR

Dr. Hossain MD. Shahin

Professor
Department of Civil and Environmental Engineering (CEE)
Islamic University of Technology (IUT)
Board Bazar, Gazipur, Bangladesh.

DECLARATION OF CANDIDATE

We hereby declare that the undergraduate research work reported in this thesis has been performed by us under the supervision of Professor Dr. Hossain MD. Shahin and this work has not been submitted elsewhere for any purpose (except for publication).

Dr. Hossain MD. Shahin

Professor,
Department of Civil and Environmental Engineering (CEE)
Islamic University of Technology (IUT)

Board Bazar, Gazipur, Bangladesh.

Date: ___/11/2017

Syed Shadman Sakib
Student No. 135412
Academic Year: 2016-2017
Date: ___/11/2017

Md. Sirajul Arefin
Student No. 135447
Academic Year: 2016-2017
Date: ___/11/2017

Asaduzzaman Chowdhury
Student No. 135416
Academic Year: 2016-2017
Date: ___/11/2017

Ferdaus Ahmmed
Student No. 135448
Academic Year: 2016-2017
Date: ___/11/2017

DEDICATION

We dedicate our thesis work to our family and some special friends who remained always beside us and continuously helped us from the backstage. A special feeling of gratitude to our loving parents.

We also dedicate this thesis to our many friends who have supported us throughout the process. We will always appreciate all they have done.

ABSTRACT

The stability of a soil slope is governed by slope geometries, stress conditions, and soil properties. External water loading, pore-pressure changes, and hydrodynamic impact from water flow are factors being either influencing, or completely governing the actual soil properties. This thesis focuses on slope stability analysis of a highway road embankment section considering impact of water level fluctuation on the stability of slope due to which soil water coupling occurs and also considering the variation in dimension of slopes. In these analyses we have done our numerical analyses with the Finite Element Method computer program named FEMtij-2D. The finite element method needs additional information regarding the potential performance of a slope but just basic parameter information is needed when we using traditional methods. A distinction should be made between drained and undrained strength of cohesive materials. Shortly, drained condition refers to the condition where drainage is allowed, while undrained condition refers to the condition where drainage is restricted. Most likely the worst case scenario occurs when the deposited water level is increased rapidly, and then the water table in the embankment is retained on an extremely high level so that the low effective stresses might lead to failure. Though, improved accessibility of high computer capacity allows for more and more advanced analyses to be carried out. In this study, advanced approaches used for soil water coupling in FEM-modeling of slope stability, were evaluated. A real slope section consisting of a well graded post-glacial till was exposed to a series of water-level fluctuation cycles. The evaluation was carried out by comparing results concerning stability, vertical displacements, pore pressures, flow, and model-parameter influence.

ACKNOWLEDGEMENTS

All the praises to Almighty Allah for giving us the opportunity to complete this book. We wish to express our sincere gratitude to Professor Dr. Hossain MD. Shahin for providing us with all the necessary facilities, giving undivided attention and fostering us all the way through the research. His useful comments, remarks and engagement helped us with the learning process throughout the thesis. We would like to express gratitude to all of the departmental faculty members for their help and support. We are also grateful to our parents for their encouragement, support and attention and for being ravished patrons.

We also place on record, our sense of gratitude to one and all, who directly or indirectly, have contributed to this venture.

TABLE OF CONTENTS

Table of contents

CHAPTER 5 CONCLUTION

Chapter 1 Introduction

1.1 General

Evaluating the stability of slopes in soil is an important, interesting, and challenging aspect of civil engineering. Slope instability is a geo-dynamic process that naturally shapes up the geo-morphology of the earth. However, they are a major concern when those unstable slopes would have an effect on the safety of people and property. Concerns with slope stability have driven some of the most important advances in our understanding of the complex behavior of soils. Extensive engineering and research studies performed over the past 70 years provide a sound set of soil mechanical principles with which to attack practical problems of slope stability.

Over the past decades, experience with the behavior of slopes, and often with their failure, has led to development of improved understanding of the changes in soil properties that can occur over time, recognition of the requirements and the limitations of laboratory and in situ testing for evaluating soil strengths, development of new and more effective types of instrumentation to observe the behavior of slopes, improved understanding of the principles of soil mechanics that connect soil behavior to slope stability, and improved analytical procedures augmented by extensive examination of the mechanics of slope stability analyses, detailed comparisons with field behavior, and use of computers to perform thorough analyses. (e.g. Lane & Griffiths, 2000; J. M. Duncan & Wright, 2005; Yang et al., 2010; Pinyol, Alonso, Corominas, & Moya, 2011; López-Acosta et al., 2013) Through these advances, the art of slope stability evaluation has entered a more mature phase, where experience and judgment, which continue to be of prime importance, have been combined with improved understanding and rational methods to improve the level of confidence that is achievable through systematic observation, testing, and analysis.

This thesis provides the comparison of different slope stability conditions considering the water level fluctuation and soil water interaction for Dhaka-Chittagong highway at a particular section. In this research we have used an elastoplastic constitutive model for

soils, called the extended subloading *tij*-model (Nakai et al., 2011) used in finite element analyses.

1.2 Background

Bangladesh has about 21,900 km of road about 65% of this network comprises rural roads. The remainder comprises both National and Regional roads in about equal proportions. This infrastructure in built using local materials which includes alluvial sands and silts, which at time contain mica and varying amount of clay, and organic materials. Substantial sections of the network are subjected to flooding for about three months annually on average. Any soil volume is continuously affected by hydrological conditions prevailing; present water is either influencing or completely governing the actual soil properties. At the scale of bank slopes and embankments, the road embankments are influenced by external water loads, development of pore pressures, and hydrodynamic impact from internal and external water flow. This internal and external water flow causing soil-water coupling. Due to soil water coupling slope stability greatly affected and in many cases slope failure may occur.

In Bangladesh Dhaka–Chittagong highway is one of the most important highway from economic perspective. Our economic development mostly depends on this highway because Dhaka–Chittagong Highway is a main transportation artery in Bangladesh, between Dhaka and Chittagong. Approximately 250 kilometers (200 miles) in length, the road links the country's two largest cities, Dhaka and Chittagong. This is the busiest road in the country and a top development priority. That’s why we consider the soil water coupling condition for the stability of the slope in this highway at Feni section.

1.3 Objective of the study

The aim of this study is to identify

1. Impact of water level fluctuation on slope stability.

2. Soil-water interaction on the slope stability.
3. Analyses of stability based on slope variability.

1.4 Scope of the study

The scope of the study may be:

1. Analyze slope stability of road embankment with different slopes.
2. Determination of optimum water level to which the slope remains stable.
3. Finding economic solutions for slope stabilization.

Chapter 2 Literature review

2.1 Ground Investigations

Before any further examination of an existing slope, or the ground onto which aslope is to be built, essential borehole information must be obtained. This information will give details of the strata, moisture content and the standing water level. Also, the presence of any particular plastic layer along which shear could more easily take place will be noted.
For the study in this thesis, we used the field data from the soil test report of the Dhaka-Chittagong highway performed at IUT Geotechnical laboratory in the previous year.

2.2 Geotechnical Parameters

Before a geotechnical analysis can be performed, the parameters values needed in the analysis must be determined.

2.2.1 Unit Weight

Unit weight of a soil mass is the ratio of the total weight of the soil to the total volume of the soil. Unit weight, γ, is usually determined in the laboratory by measuring the weight and volume of a relatively undisturbed soil sample obtained from the field. Measuring unit weight of soil directly in the field might be done by sand cone test, rubber balloon or nuclear densiometer. We will use unit weights presented in a report by IUT Geotechnical laboratory.

2.2.2 Cohesion

Cohesion, c, is usually determined in the laboratory from the Direct Shear Test. Unconfined Compressive Strength S_u can be determined in the laboratory using the Triaxial Test or the Unconfined Compressive Strength Test. There are also correlations for S_u with shear strength as estimated from the field using Vane Shear Tests. Our soil test report has already determined the cohesions for this project.

2.2.3 Friction Angle

The angle of internal friction, φ, can be determined in the laboratory by the Direct Shear Test or by Triaxial test. For our analysis we will use values determined by IUT Geotechnical laboratory soil test report.

2.2.4 Young's Modulus of Soil

Young's soil modulus, E_s , may be estimated from empirical correlations, laboratory test results on undisturbed specimens and results of field tests. Laboratory test that might be used to estimate the soil modulus is the triaxial test. For our analysis we will use values determined by IUT Geotechnical laboratory soil test report.

2.3 Type of soil

Geotechnical engineers classify soils, or more properly earth materials, for their properties relative to foundation support or use as building material. These systems are designed to predict some of the engineering properties and behavior of a soil based on a few simple laboratory or field tests.

2.3.1 Sand

Soil material that contains 85% or more sand; the percentage of silt plus 1.5 times the percentage of clay does not exceed 15 (CSSC; USDA).

2.3.2 Clay

Soil material that contains 40% or more clay and 40% or more silt (CSSC; USDA).

2.3.3 Silty clay

Soil material that contains 40% or more clay and 35% or more silt (CSSC; USDA).

2.3.4 Silt

Soil material that contains 80% or more silt and less than 12% clay (CSSC; USDA).

2.3.5 Sandy clay

Soil material that contains 7 to 27% clay, 28 to 50% silt, and less than 52% sand (CSSC; USDA).

2.4 Basic Requirement for Slope Stability Analysis

Whether slope stability analyses are performed for drained conditions or undrained conditions, the most basic requirement is that equilibrium must be satisfied in terms of total stresses. All body forces (weights), and all external loads, including those due to water pressures acting on external boundaries, must be included in the analysis. These analyses provide two useful results: (1) the total normal stress on the shear surface and (2) the shear stress required for equilibrium.

The factor of safety for the shear surface is the ratio of the shear strength of the soil divided by the shear stress required for equilibrium. The normal stresses along the slip surface are needed to evaluate the shear strength: except for soils with $\varphi = 0$, the shear strength depends on the normal stress on the potential plane of failure.

In effective stress analyses, the pore pressures along the shear surface are subtracted from the total stresses to determine effective normal stresses, which are used to evaluate shear strengths. Therefore, to perform effective stress analyses, it is necessary to know (or to estimate) the pore pressures at every point along the shear surface. These pore pressures can be evaluated with relatively good accuracy for drained conditions, where their values

are determined by hydrostatic or steady seepage boundary conditions. Pore pressures can seldom be evaluated accurately for undrained conditions, where their values are determined by the response of the soil to external loads.

In total stress analyses, pore pressures are not subtracted from the total stresses, because shear strengths are related to total stresses. Therefore, it is not necessary to evaluate and subtract pore pressures to perform total stress analyses. Total stress analyses are applicable only to undrained conditions. The basic premise of total stress analysis is this: the pore pressures due to undrained loading are determined by the behavior of the soil. For a given value of total stress on the potential failure plane, there is a unique value of pore pressure and therefore a unique value of effective stress. Thus, although it is true that shear strength is really controlled by effective stress, it is possible for the undrained condition to relate shear strength to total normal stress, because effective stress and total stress are uniquely related for the undrained condition. Clearly, this line of reasoning does not apply to drained conditions, where pore pressures are controlled by hydraulic boundary conditions rather than the response of the soil to external loads.

2.5 Analyses of Drained Conditions

Drained conditions are those where changes in load are slow enough, or where they have been in place long enough, so that all of the soils reach a state of equilibrium and no excess pore pressures are caused by the loads. In drained conditions pore pressures are controlled by hydraulic boundary conditions. The water within the soil may be static, or it may be seeping steadily, with no change in the seepage over time and no increase or decrease in the amount of water within the soil. If these conditions prevail in all the soils at a site, or if12the conditions at a site can reasonably be approximated by these conditions, a drained analysis is appropriate. A drained analysis is performed using:

- Total unit weights
- Effective stress shear strength parameters
- Pore pressures determined from hydrostatic water levels or steady seepage analyses.

2.6 Analyses of Undrained Conditions

Undrained conditions are those where changes in loads occur more rapidly than water can flow in or out of the soil. The pore pressures are controlled by the behavior of the soil in response to changes in external loads. If these conditions prevail in the soils at a site, or if the conditions at a site can reasonably be approximated by these conditions, an undrained analysis is appropriate. An undrained analysis is performed using.

- Total unit weights
- Total stress shear strength parameters

2.7 Short-Term Analyses

Short term refers to conditions during or following construction—the time immediately following the change in load. For example, if constructing a sand embankment on a clay foundation takes two months, the short-term condition for the embankment would be the end of construction, or two months. Within this period of time, it would be a reasonable approximation that no drainage would occur in the clay foundation, whereas the sand embankment would be fully drained.

2.8 Long-Term Analyses

After a period of time, the clay foundation would reach a drained condition, and the analysis for this condition would be performed as discussed earlier under ‘‘Analyses of Drained Conditions’’, because long term and drained conditions carry exactly the same meaning. Both of these terms refer to the condition where drainage equilibrium has been reached and there are no excess pore pressures due to external loads.

2.9 Pore Water Pressures

For effective stress analyses the basis for pore water pressures should be described. If pore water pressures are based on measurements of groundwater levels in bore holes or with piezometers, the measured data should be described and summarized in appropriate figures or tables. If seepage analyses are performed to compute the pore water pressures, the method of analysis, including computer software, which was used, should be described. Also, for such analyses the soil properties and boundary conditions as well as any assumptions used in the analyses should be described. Soil properties should include the hydraulic conductivities. Appropriate flow nets or contours of pore water pressure, total head, or pressure head should be presented to summarize the results of the analyses.

2.10 Soil Property Evaluation

The basis for the soil properties used in a stability evaluation should be described and appropriate laboratory test data should be presented. If properties are estimated based on experience, or using correlations with other soil properties or from data from similar sites, this should be explained. Results of laboratory tests should be summarized to include index properties, water content, and unit weights. For compacted soils, suitable summaries of compaction moisture–density data are useful. A summary of shear strength properties is particularly important and should include both the original data and the shear strength envelopes used for analyses (Mohr–Coulomb diagrams, modified Mohr–Coulomb diagrams). The principal laboratory data that are used in slope stability analyses are the unit weights and shear strength envelopes. If many more extensive laboratory data are available, the information can be presented separately from the stability analyses in other sections, chapters, or separate reports. Only the summaries of shear strength and unit weight information need to be presented with the stability evaluation in such cases.

2.11 Circular Slip Surface

Inherent in limit equilibrium stability analyses is the requirement to analyze many trials slip surfaces and find the slip surface that gives the lowest factor of safety. Included in this trial approach is the form of the slip surface; that is, whether it is circular, piece-wise linear or some combination of curved and linear segments. Slope/W has a variety of options for specifying trial slip surfaces (Bishop, A. (1955)) The position of the critical slip surface is affected by the soil strength properties. The position of the critical slip surface for a purely frictional soil (c = 0) is radically different than for a soil assigned untrained strength (φ = 0). This complicates the situation, because it means that in order to find the position of the critical slip surface, it is necessary to accurately define the soil properties in terms of effective strength parameters.

2.12 Factor of Safety

In slope stability, and in fact generally in the area of geotechnical engineering, the factor which is very often in doubt is the shear strength of the soil. The loading is known more accurately because usually it merely consists of the selfweight of the slope. The FoS is therefore chosen as a ratio of the available shear strength to that required to keep the slope stable. For highly unlikely loading conditions, accepted factors of safety can be as low as

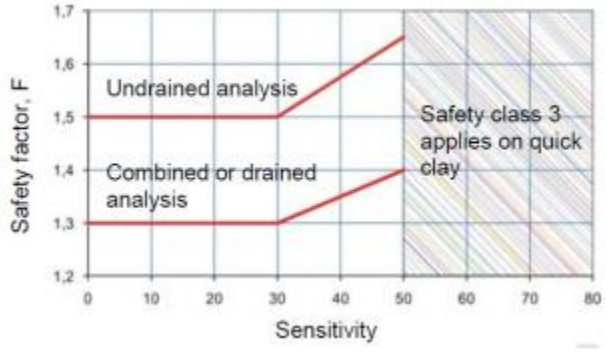

Figure 4.1: The minimum acceptable safety factor value for geotechnical structures on safety class 2 clay according to TK Geo 11

1.2-1.25, even for dams e.g. situations based on seismic effects, or where there is rapid

drawdown of the water level in a reservoir. According to TK Geo 11(Swedish Transport Administration requirements and guidelines) allowable limit for factor of safety is 1.5 for undrained analysis and 1.3 for combined or drained analysis.

2.13 Traffic load

Traffic load refers to the action of the traffic on the carriageway or railway structure. Action distribution shall be taken into consideration using an elastic theoretical based method. Where there are low permeable soils the traffic load is to be reduced for drained and combined analysis. Normally the traffic load can be ignored for combined analysis and drained analysis in the above conditions. Account must be taken of the vehicles and other equipment used in the execution phase.

Design using partial factors. The characteristic surface load for traffic shall be:

- 15 kN/m2 for design situations where the critical failure surfaces are short
- 10 kN/m2 for design situations where the critical failure surfaces are long Design using characteristic values. The characteristic surface load for traffic shall be:
- 20 kN/m2 for design situations where the critical failure surfaces are short
- 13 kN/m2 for design situations where the critical failure surfaces are long

2.14 Numerical analysis

Slope stability analyses can be performed using deterministic or probabilistic input parameters. FEMtij-2D can model isoparametric soil types, complex stratigraphic and slip surface geometry, and variable pore-water pressure conditions using a large selection of soil models.

Chapter 3 Methodology

Many different solution techniques for slope stability analyses have been developed over the years. Analyze of slope stability is one of the oldest type of numerical analysis in geotechnical engineering. In this project we will use Finite Element Method for our analysis. FEMtij-2D a geotechnical finite element analysis software for 2D static analysis developed by Professor Dr. Hossain MD. Shahin at Nagoya Institute of Technology, Nagoya.

3.1 Finite Element Modeling

The finite element program FEMtij-2D was used for evaluating the stability of embankment slope. The road embankment cross-section utilized for the numerical model is presented in figure 3.1

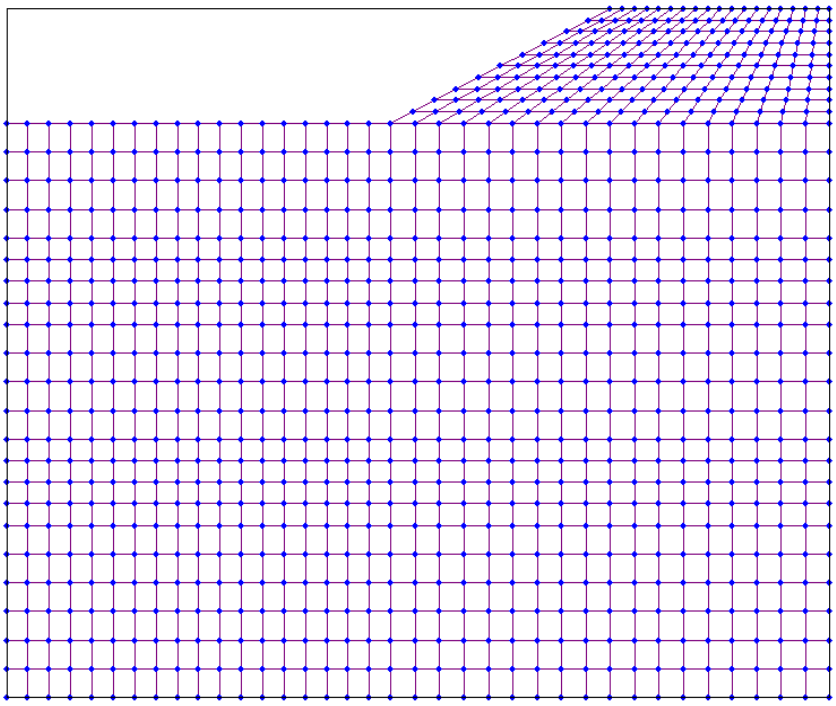

Figure 3.1: Left half of the embankment cross-section mesh

3.2 Mesh Generation and Boundary Conditions

In this modeling, 4-node rectangular elements were used; see figure 3.1. The powerful 4-node element provides an accurate calculation of stresses and failure loads. The two vertical boundaries are free to move vertically only supported as roller support at the left and right side of the embankment as shown in figure 3.2, whereas the horizontal boundary at the bottom is considered to be pinned support.

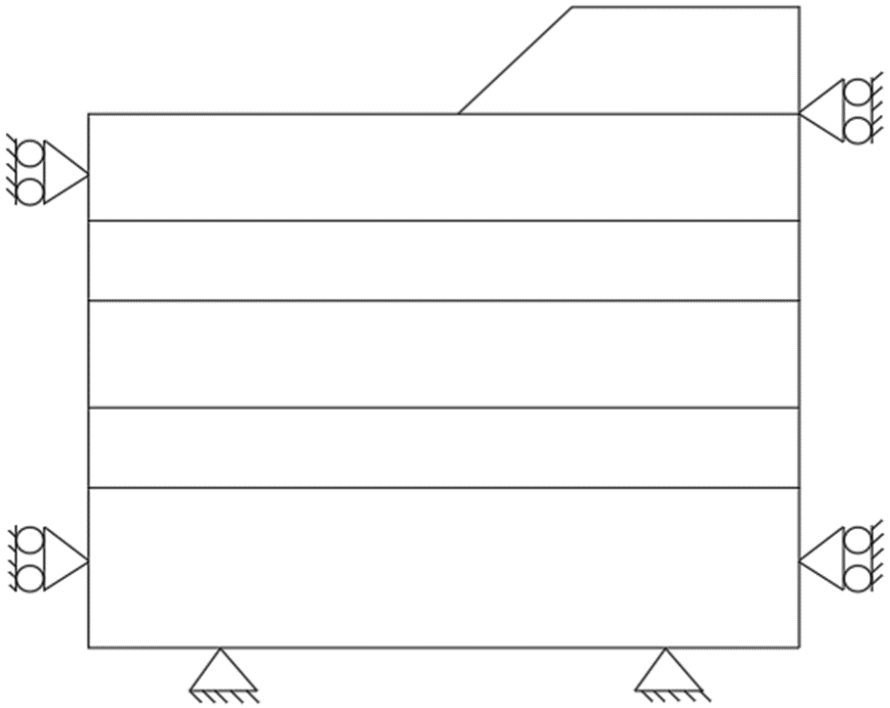

Figure 3.2: Boundary conditions used in analysis

3.3 Material Model

In this research, two-dimensional finite element anlayses were carried out with an academic program called FEMtij-2D, using the elastoplastic subloading tij model . This model can describe the typical stress, deformation and strength characteristics of soils, such as the

influence of the intermediate principal stress, the influence of stress-path dependency of the plastic flow and the influence of the density and/or the confining pressure.

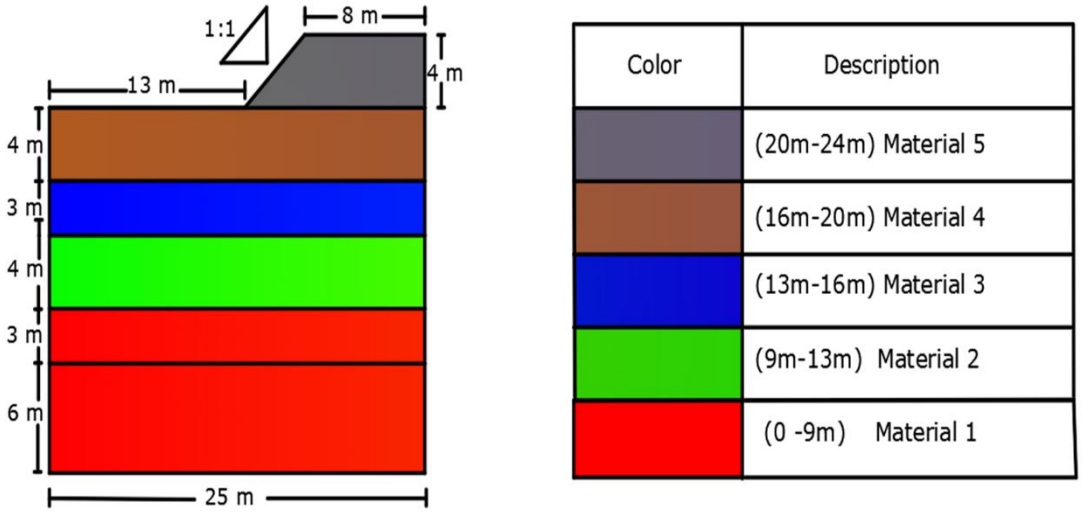

Figure 3.3: Materials used in different layers.

Table 3.1 Used parameters for subloading tij model.

Parameter	Notation	Value			Remarks
		Layer 1 Depth (m): 0-5	Layer 2 Depth (m): 5-9	Layer 3 Depth (m): 9-18	
Compression index	λ	0.1038	0.1-018	0.0819	Same parameters as cam-clay model
Swelling index	k	0.00829	0.00803	0.00983	
Reference void ratio on normally consolidation line at P=98 kPa & q=0 kPa	N	0.865	0.868	0.778	
Critical stress ratio	$R_{CS}=(\sigma_1/\sigma_2)_{CS}$ (comp)	3.98	4.00	4.00	
Poisson's ratio	μ	0.2	0.2	0.2	
Shape of yield surface (same as original cam clay at β=1)	β	1.60	1.60	1.60	
Influence of density and confining pressure	a	800	850	800	

3.4 Drainage Boundary Conditions

The model used here has 2 types of drainage boundary conditions. The left, right and the bottom of the cross-section was modelled as undrained boundary and the top level where the water level fluctuates is modelled as drained boundary to represent the actual situations. Figure 3.4 shows the water level fluctuation and drainage boundary changes.

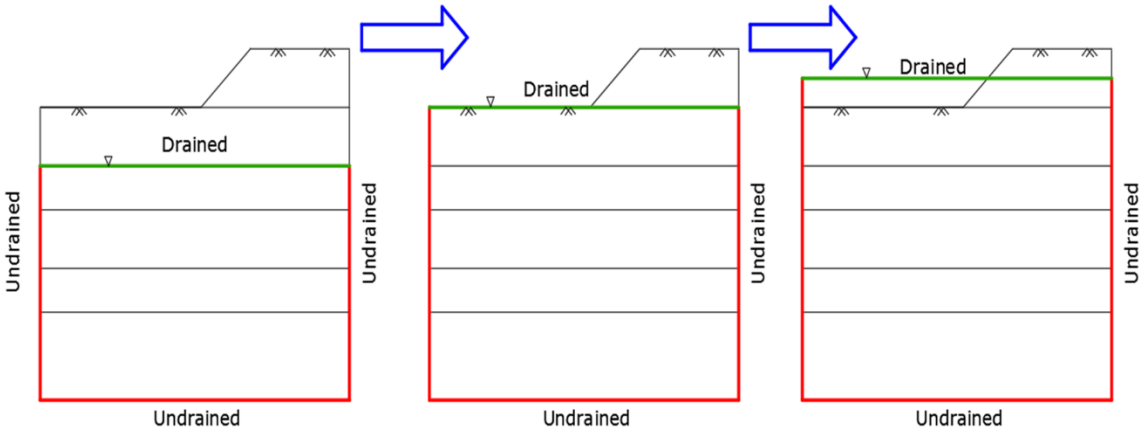

Figure 3.4: Water level fluctuation and drainage boundary conditions.

3.5 Simulated Models

We have used 4 different models for determining the suitable condition for embankment design. Different models have different slopes and water level conditions. Figure 3.5 shows the specifications for the

Case	Water Level	Slope(V:H)
Case1	Up to surface	1:1
Case2	Up to half of road embankment	1:1
Case3	Up to half of road embankment	1:1.5
Case4	Up to half of road embankment	1:2

Chapter 4 Results and Discussion

4.1 Initial Ground Condition

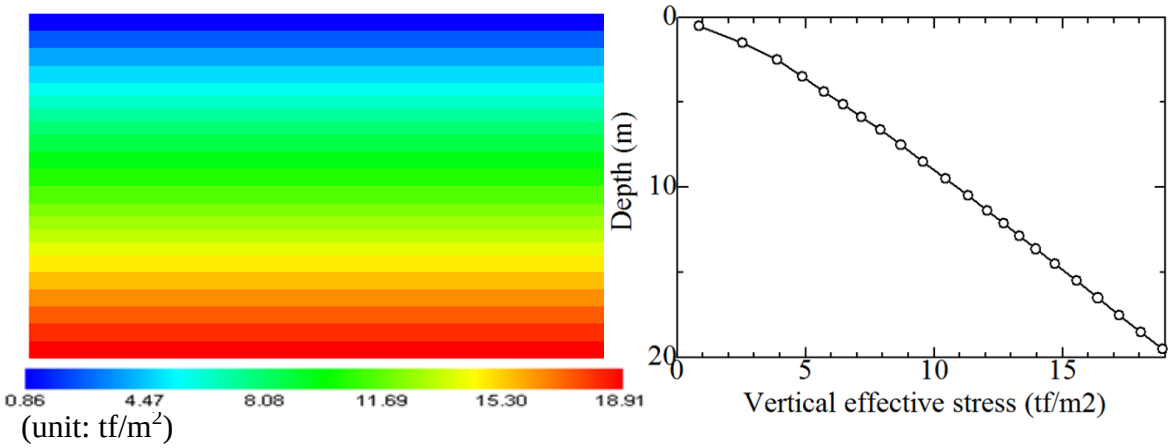

Figure 4.1: Initial Vertical stress distribution

The base of the embankment has different soil layers. The vertical stress increases as depth increases as the results show in figure 4.1. These figures show the initial condition of the ground when the embankment was not created and the water level was up to the third layer of soil from the bottom of the embankment. Also the figure 4.2 shows the coefficient of earth pressure at rest K_0 and void ratio plot for the initial ground condition.

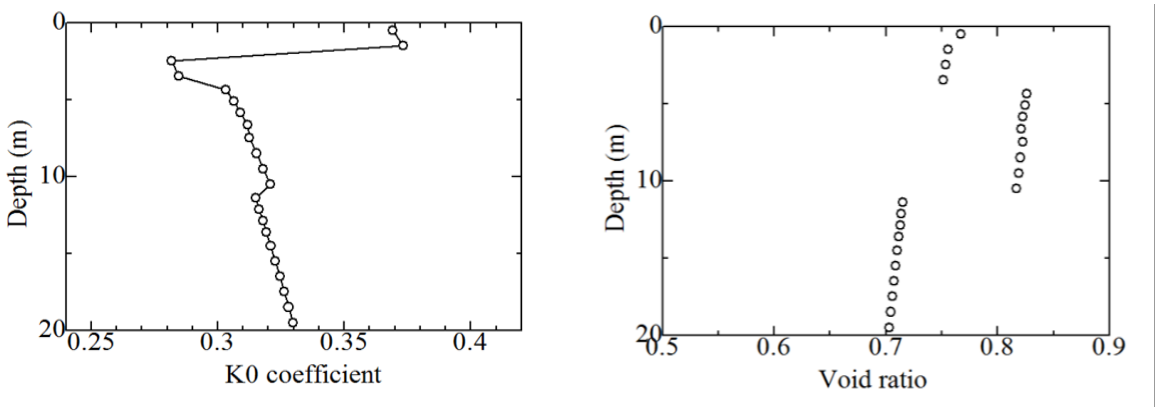

Figure 4.2: K_0 coefficient and void ratio plot for initial ground

4.2 Analysis of Case No. 1

Case no. 1 consists of 1:1 slope. This case represents the actual slope of the Dhaka-Chittagong highway that was built. We have considered the water level rise for this case is up to the surface of the ground.

4.2.1 Vertical Stress (Case 1)

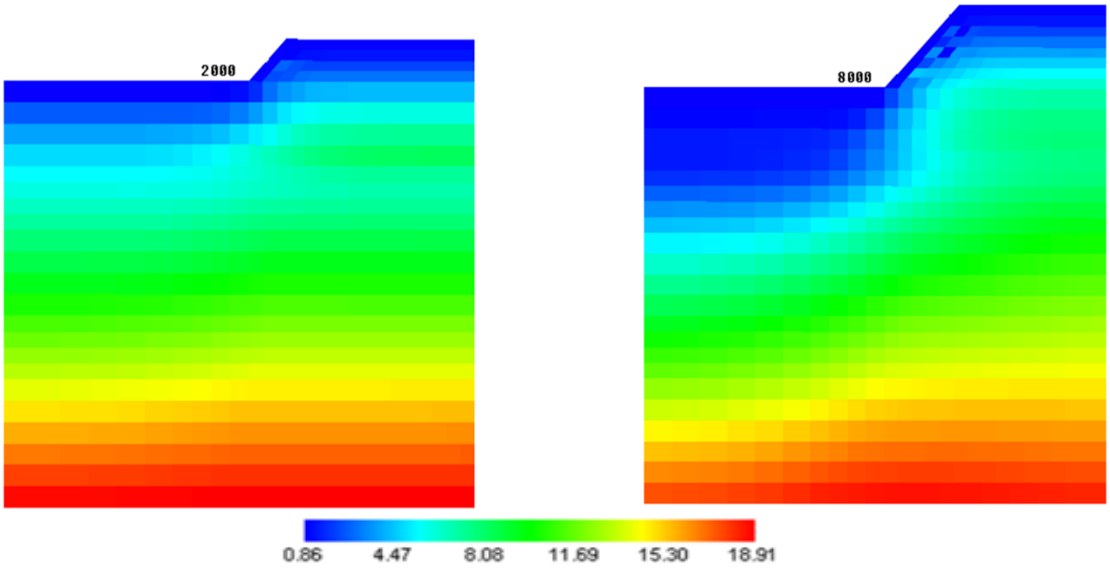

(a) Embankment Height: 2.0 m (b) Embankment Height: 4.0 m

Figure 4.3: Distribution of vertical stress at different stages: unit (tf/m^2)

As the construction of the embankment proceeds the vertical stress distribution in the ground as well as the embankment also changes. Figure 4.3 shows the change of the vertical stress at two different stages. The first figure is the condition when the half of the embankment construction is complete and the second figure is for the completed embankment. Vertical stress increases as the embankment soil filling proceeds. Vertical stress is greater below the embankment.

4.2.2 Shear Strain (Case 1)

Soil particles hold up itself with the shear strength between the soil particles. Shear strain diagram shows the most strained zones where the probable shear failure may occur and for the case no. 1 the toe of the embankment is the most critical zone. It has a maximum shear strain of .037 just a bit right of the toe of the embankment. Figure 4.4 shows the simulated shear strain diagram for case no. 1.

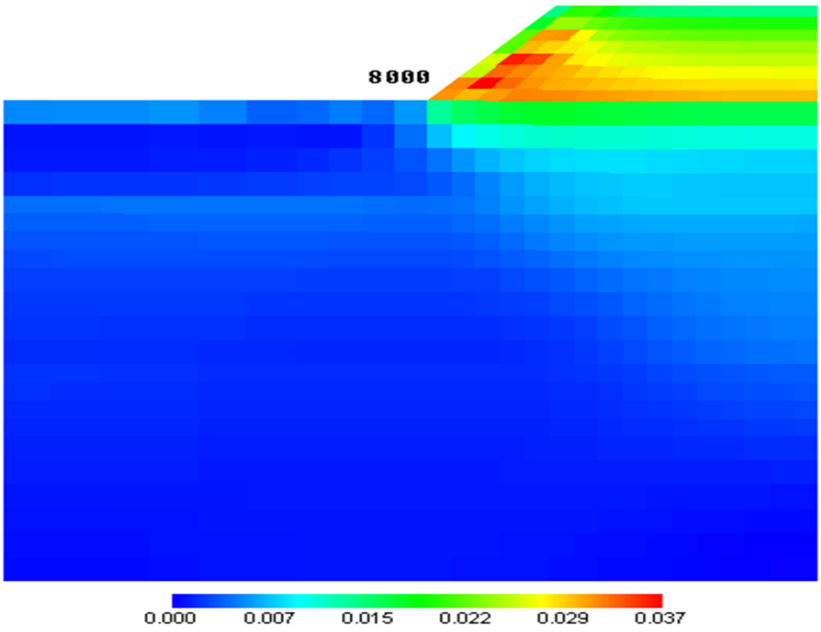

Figure 4.4: Distribution of shear strain for case no. 1 (after 740 days)

4.2.3 Effective Pore Water Pressure (Case 1)

For case no. 1 the water level was risen up to the surface level. As a result, pore water pressure has been developed only at the base and it is maximum below the embankment. The embankment itself has zero pore water pressure and the value of maximum pore water pressure at base is 4.15 tf/m^2. Figure 4.5 show the result of pore water pressure for case no.1

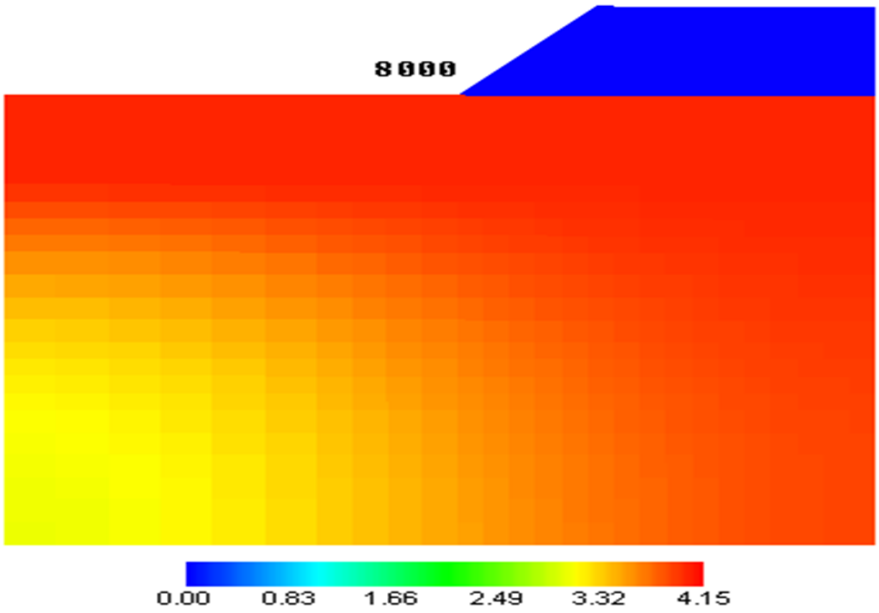

Figure 4.5: Distribution of pore water pressure for case no. 1-(unit: tf/m^2, after 740 days)

4.2.4 Displacement Vector (Case1)

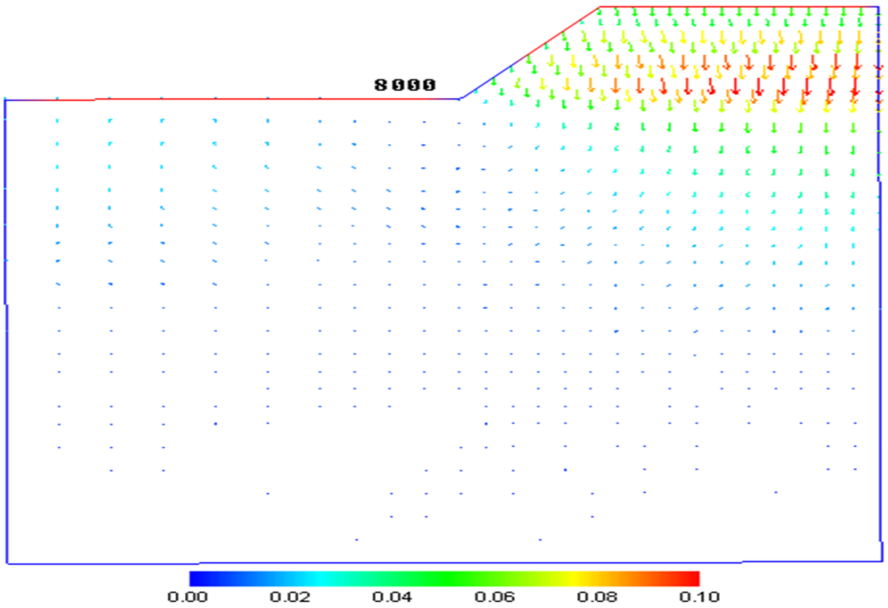

Figure 4.6: Distribution of vertical displacement vector: (unit : meter, after 740 days)

In figure 4.6 the displacement vector for case no. 1 shows that the embankment is stable and the soil particles are settling downwards. Stabilization of the soil particles is also understood form the displacement vector. It has a maximum value of 10 cm in the embankment just at the top of the base level.

4.2.5 Surface Settlement (Case1)

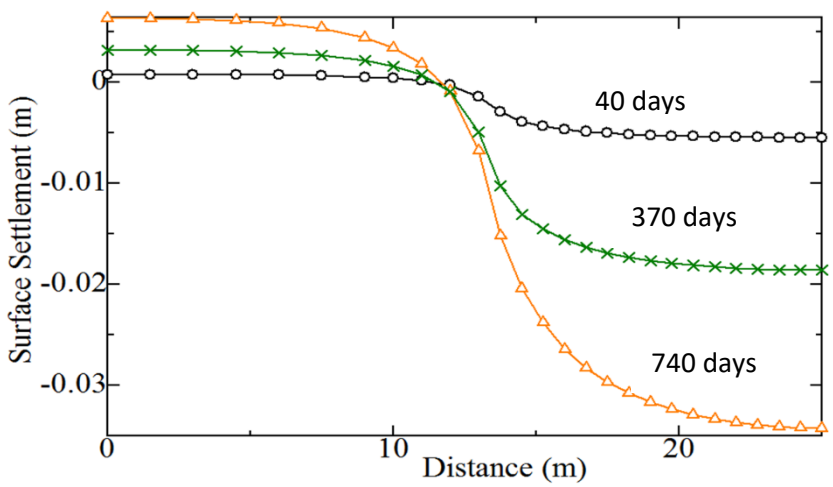

Figure 4.7: Plot for surface settlement at different stages. (case1)

The plot in figure 4.7 shows the settlement of the base surface with respect to time. 3 different time periods show that maximum settlement after about 2 years is 3cm at a middle of the cross section of the base. This settlement is due to the self-weight of the embankment. There is some negative or upward movement of the base at the left most corner due to the concentration of load at the middle of the embankment.

4.3 Analysis of Case No. 2

Case no. 2 consists of 1:1 slope and the water level this time has been risen up to the half of the embankment. A slope of 1:1 is not suitable for this much water level rise and the

simulation results show the failure of the slope when water level is risen. The detailed results are discussed below.

4.3.1 Vertical Stress (Case 2)

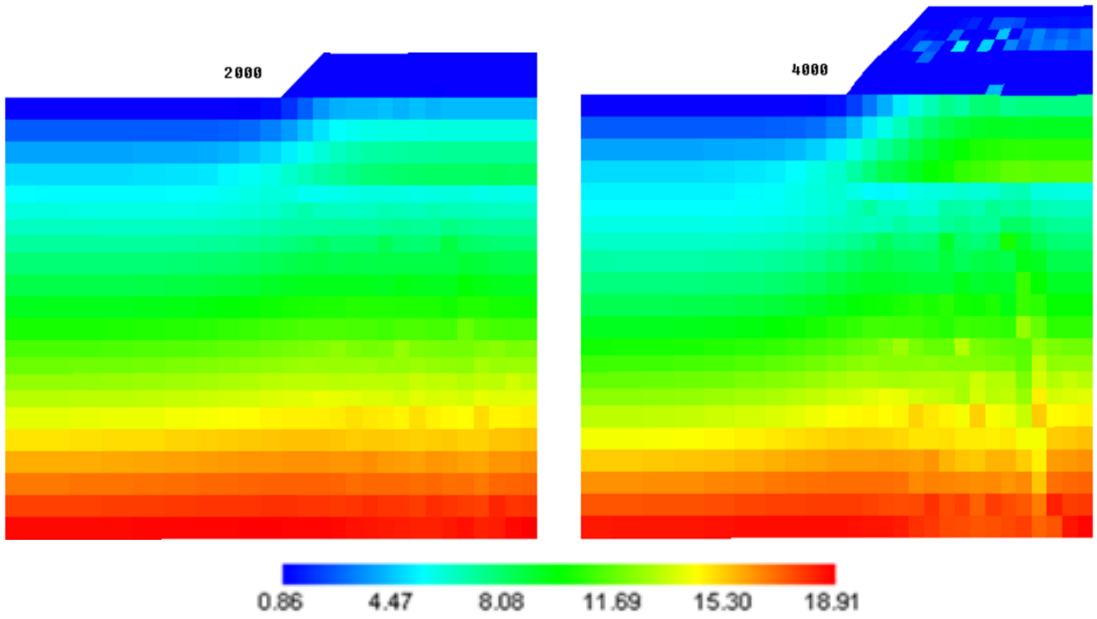

(a) After 185 days (b) after 370 days

Figure 4.8: Distribution of vertical stress at different stages for Case 2 (unit: tf/m^2)

As water level is risen up to the half of the embankment there is actually very few significant amount of change in the vertical stress distribution. The bottom of the bas has the maximum vertical stress developed which is about 18.91 tf/m^2. The figure 4.8 shows the change of the vertical stress distribution of the cross-section during half and full stage of the construction of the embankment. Figure 4.9 shows the vertical stress distribution when the embankment has failed. Stress has been released in the top level of the cross-section when the failure has occurred.

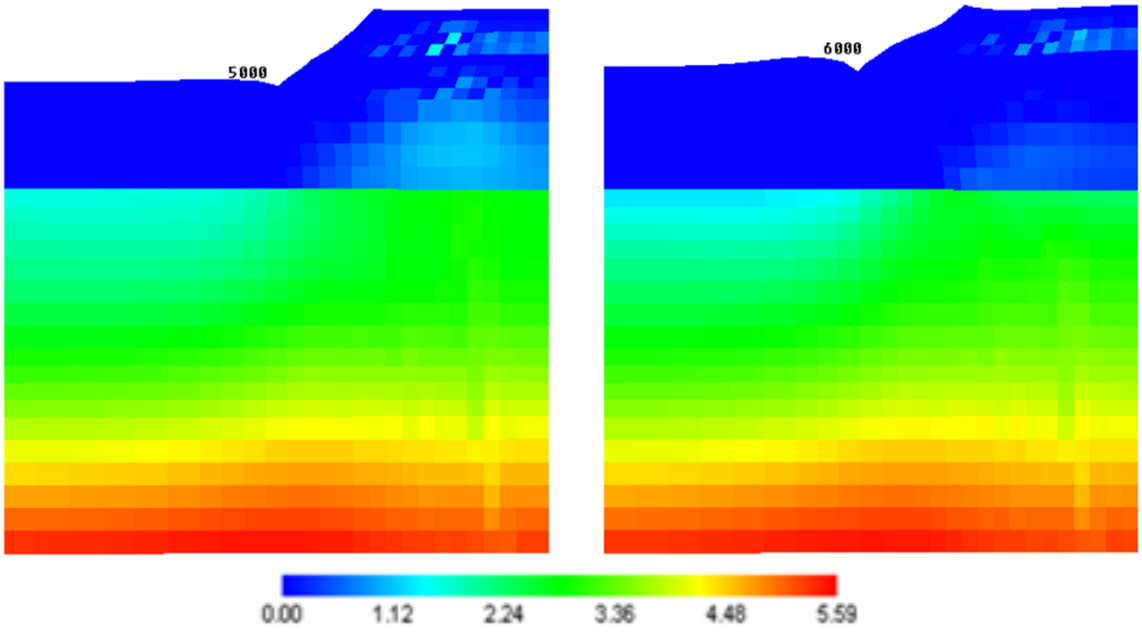

(a) after 465 days (b) after 555 days

Figure 4.9: Distribution of vertical stress at different stages (Case 2): unit (tf/m^2)

4.3.2 Pore Water Pressure (Case 2)

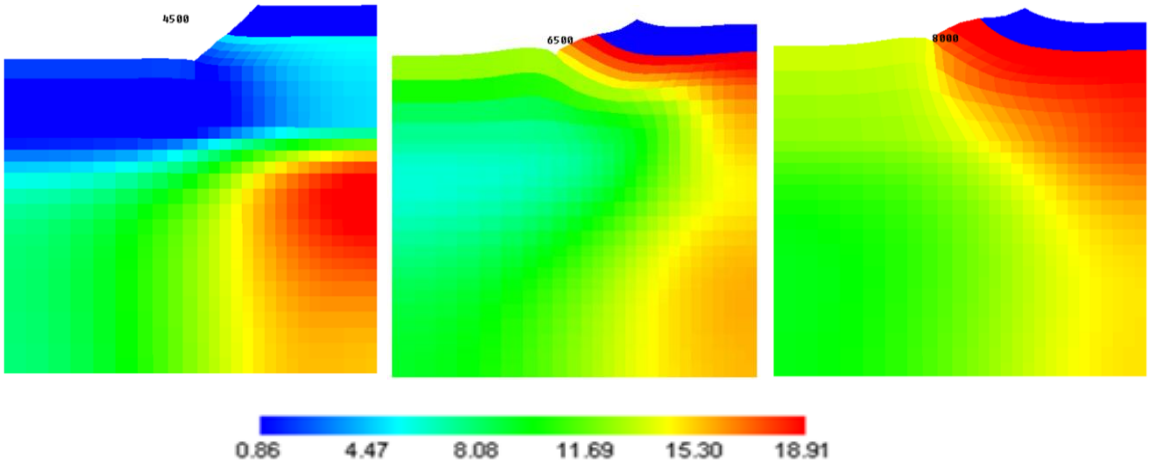

(a) after 420 days (b) after 602 days (c) after 740 days

Figure 4.10: Distribution of pore water pressure with time for Case 2: (unit: tf/m^2)

Simulation results show that with time excess pore water pressure has been developed at center of the base below the embankment. Also the pore water is maximum just at the bottom portion of the embankment when the slope is at failure condition. The maximum pore water pressure developed for case no. 2 is greater than in the case no. 1. The maximum value of pore water pressure for case no. 2 is 5.59 tf/m^2. Figure 4.10 describes the simulated results of pore water pressure for case no. 2.

4.3.3 Displacement Vector (Case2)

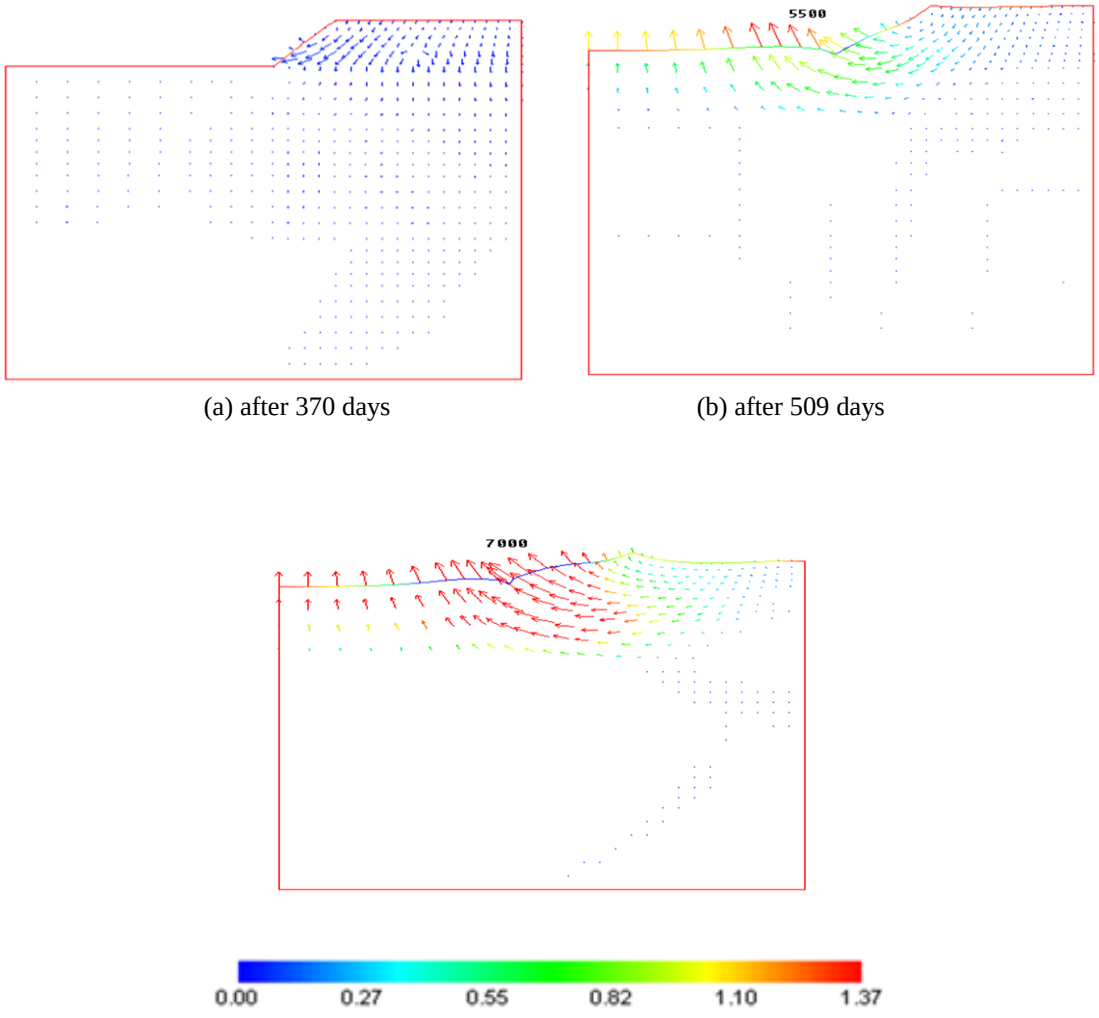

(a) after 370 days

(b) after 509 days

(c) after 740 days

Figure 4.11: Displacement vector with time (case 2): unit (meter)

Figure 4.11 presents displacement vector that shows the gradual failure of the slope when water level is risen up to the half of the embankment. The slope becomes unstable as water level is increased. Lateral displacement of the toe of the slope causes the total slope failure.

4.3.4 Surface Settlement (Case2)

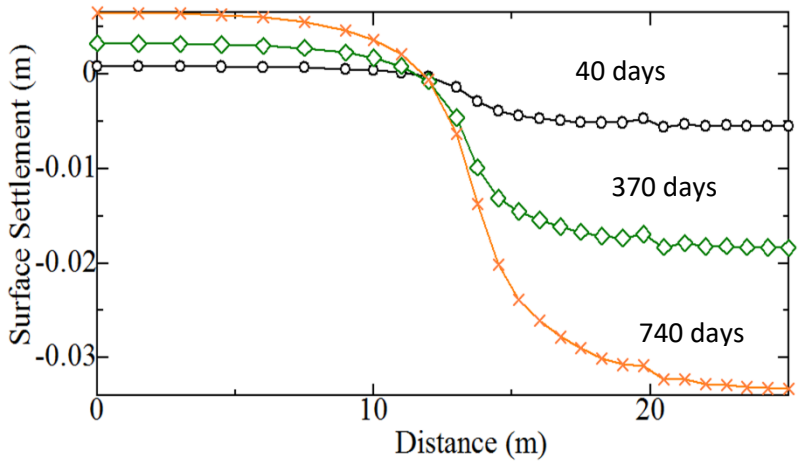

Figure 4.12: Plot for surface settlement at different stages (case2).

Surface settlement plot for the base is shown in figure 4.12. There is very little difference in the surface settlement compared to case 1. No significant effect is seen in the base settlement due to the water level rise as the slope remains as 1:1 similar to case 1. The place where the embankment is made has a maximum 3.5 cm settlement in two years. The left side of the embankment has some amount of negative or upward thrust due to the embankment load applied to the base.

4.4 Analysis of Case 3

Case has been set up with a slope of 1:1.5 (V:H) and the water level is kept at the half of the embankment to check if the failure could be stopped by increasing the horizontal component of the slope. But 1:1.5 slope was not enough stable to resist the failure of the slope.it has also failed when the water level has been increased to half of the embankment. Detailed results discussed below.

4.4.1 Vertical Stress (Case 3)

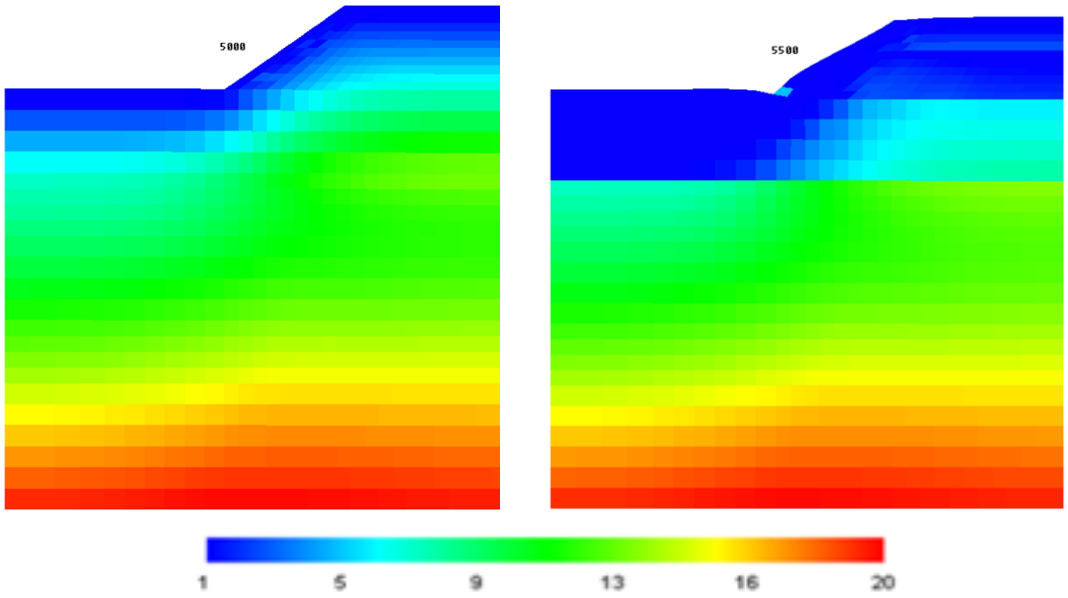

Figure 4.13: Distribution of vertical stress at different stages (Case 3): unit (tf/m^2)

Due to the change of the slope of the embankment this time there is some amount of increase in the vertical stress of the cross-section. Vertical stress has been increased by 10% compared to the case 1. Figure 4.13 shows the change of the vertical stress in the cross-section. Maximum value of vertical stress is at the bottom of the base and its value

is 20 tf/m^2. Although the slope has failed when water level is increased but it has proved the improvement of slope failure due to increase of the horizontal component of the slope.

4.4.2 Pore Water Pressure (Case 3)

There is significant change in the pore water pressure development due to the increase of the slopes horizontal component. There is no excess pore water pressure present in the embankment and also the first layer of base. Figure 4.14 show the change of pore water

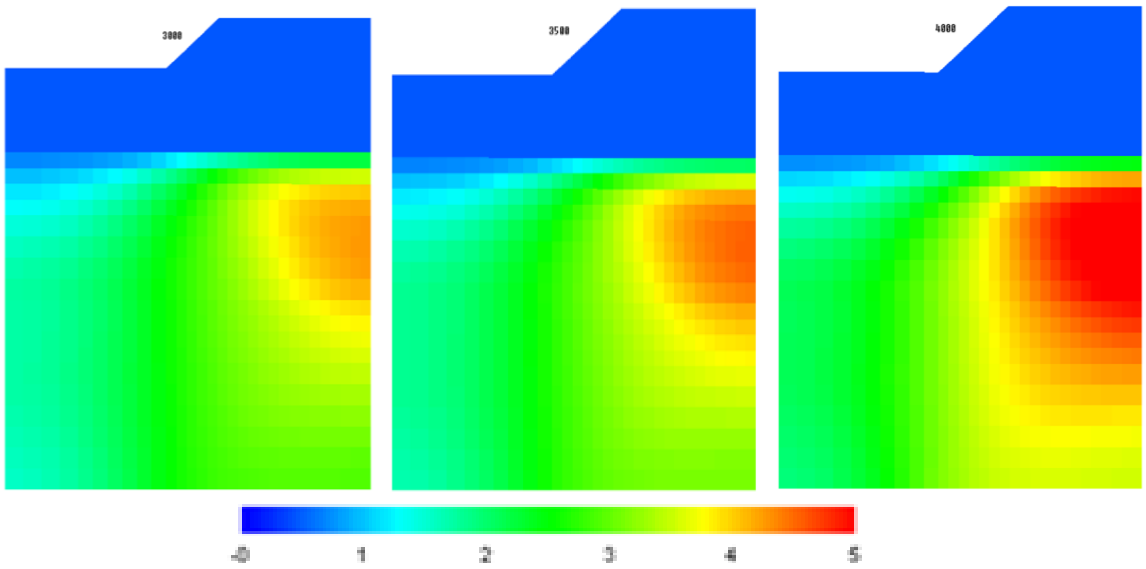

(a) after 185 days (b) after 232 days (c) after 370 days

Figure 4.14: Distribution of pore water pressure with time (case 3): unit (tf/m^2).

pressure. Below the embankment there is the maximum pore water pressure developed in the base which is also 5% less than of case 1. It signifies the improvement of slope failure.

4.4.3 Displacement Vector (Case3)

Case 3 has a better stabilization than case 1 and case 2 where the slope was 1:1. Displacement vector diagram shows that increasing the slope increases the stability of the slope. The direction of the soil particles movement has now been lowered which is a very good news. Although it didn't completely stop slope failure but it has significantly improved the condition.

Before failure maximum settlement was found in the embankment. But as the slope started to fail then the lateral displacement of the soil particles at the toe of the embankment has started to initialize the slope failure.

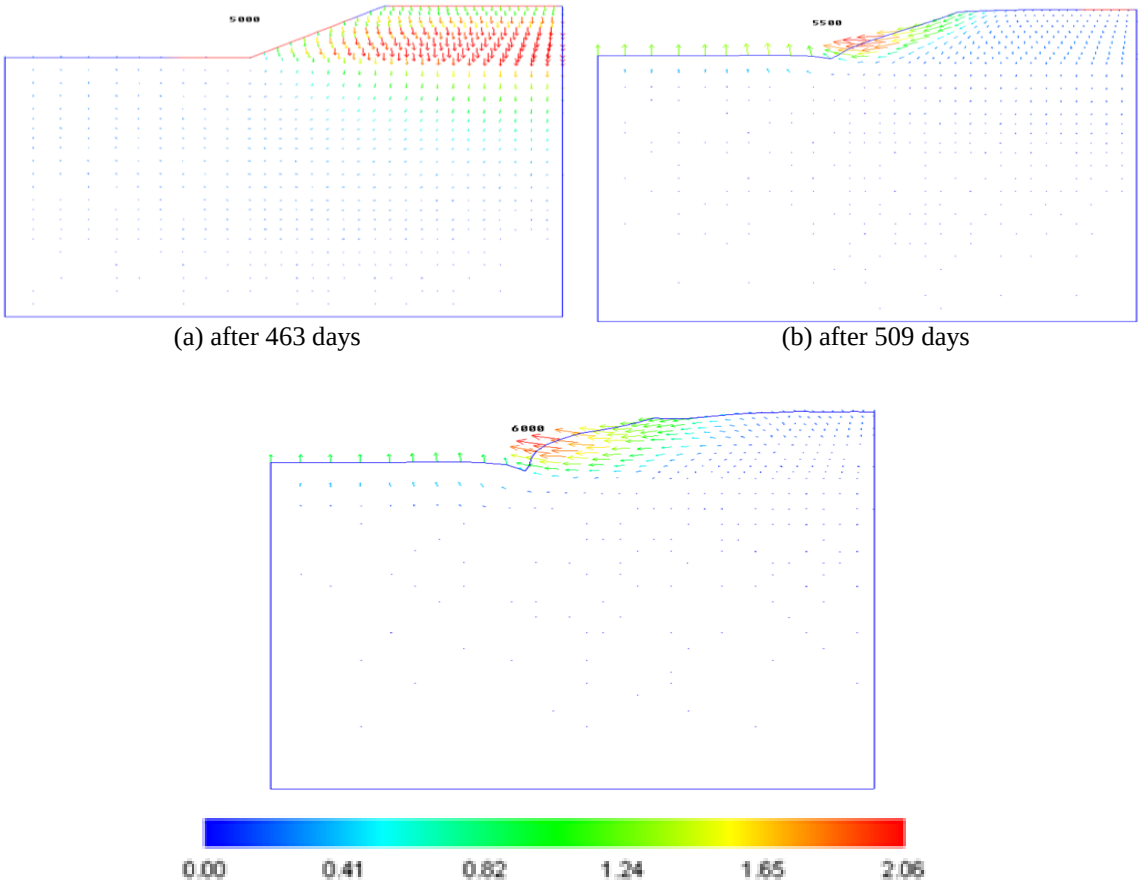

(a) after 463 days

(b) after 509 days

(c) after 555 days

Figure 4.15: Displacement vector with time (case 3): unit (meter)

4.4.4 Surface Settlement (Case 3)

Plot of the surface settlement shows the settlement of the surface of the base. Due to the change of the slope there is significant amount of change in the surface settlement for case 3 as compared to case1 and case 2. The amount of settlement after two years is almost doubled. This means the embankment has stabilized successfully. Though the water level rise caused the slope to fail but the change of the slope has the improvement in stabilization which was necessary for the stability of the slope. Figure 4.16 shows the surface settlement.

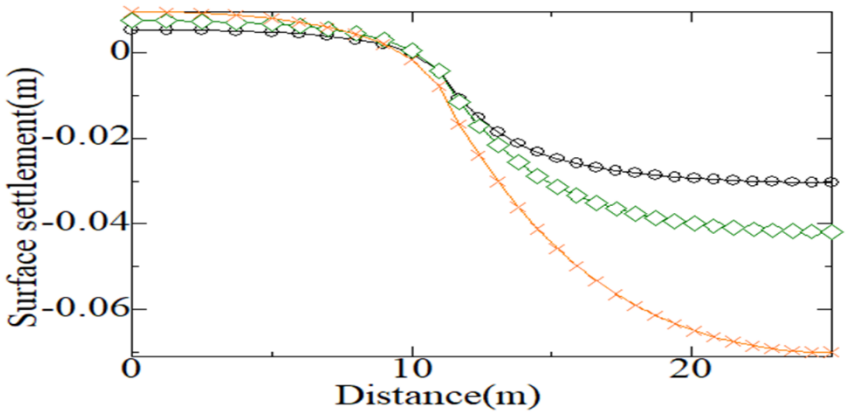

Figure 4.16: Plot for surface settlement at different stages (case3).

4.5 Analysis of Case No. 4

Case 4 consists of a slope of 1:2 (V:H). It performs better than all the other 3 cases. It has a better stabilization and a greater stability all the way. The pore water pressure development has also been decreased significantly for this slope. Analysis results for case 4 are discussed below in details.

4.5.1 Vertical Stress (Case 4)

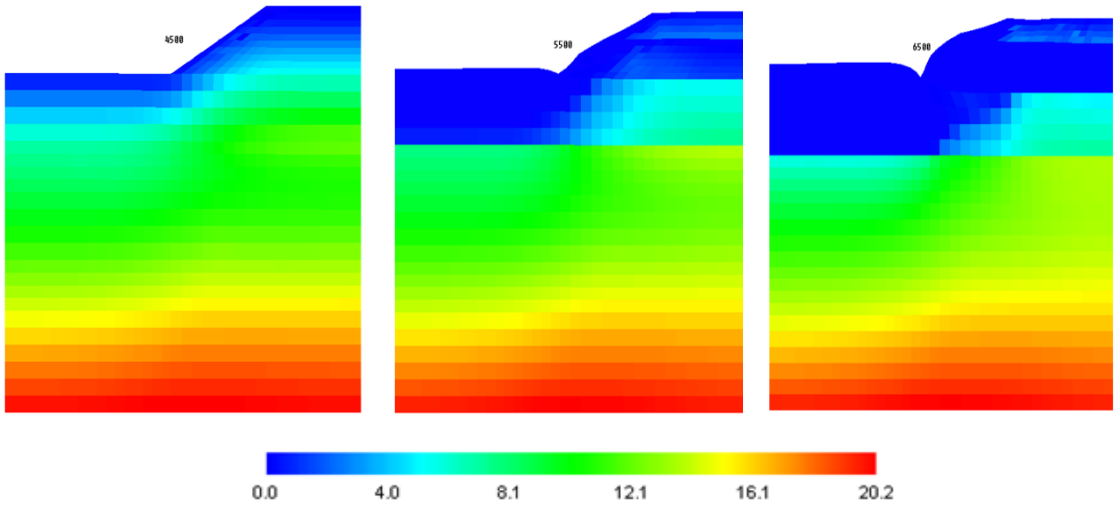

(a) after 417 days (b) after 509 days (c) after 740days

Figure 4.17: Distribution of vertical stress at different stages (Case 4): unit (tf/m^2)

Vertical stress has been increased by 13% in case 4 as compared to case 1 and case 2. The bottom of the cross-section has the maximum vertical stress of 20.2 tf/m^2 . The place where the embankment is created over the base has a greater value of vertical stress. This slope is better than any other slopes analyzed before. Though the slope has ultimately failed but it showed a greater resistance before failure.

4.5.2 Shear Strain (Case 4)

Shear strain diagram shows the most strained zones where the probable shear failure may occur and for the case no. 1 the toe of the embankment is the most critical zone. It has a maximum shear strain of .045 just a bit right of the toe of the embankment. Figure 4.18 shows the simulated shear strain diagram for case no. 4. Shear strain for case 4 is much greater than case 1. This indicates the flexibility of the slope which is better than 1:1 and 1:1.5 slope.

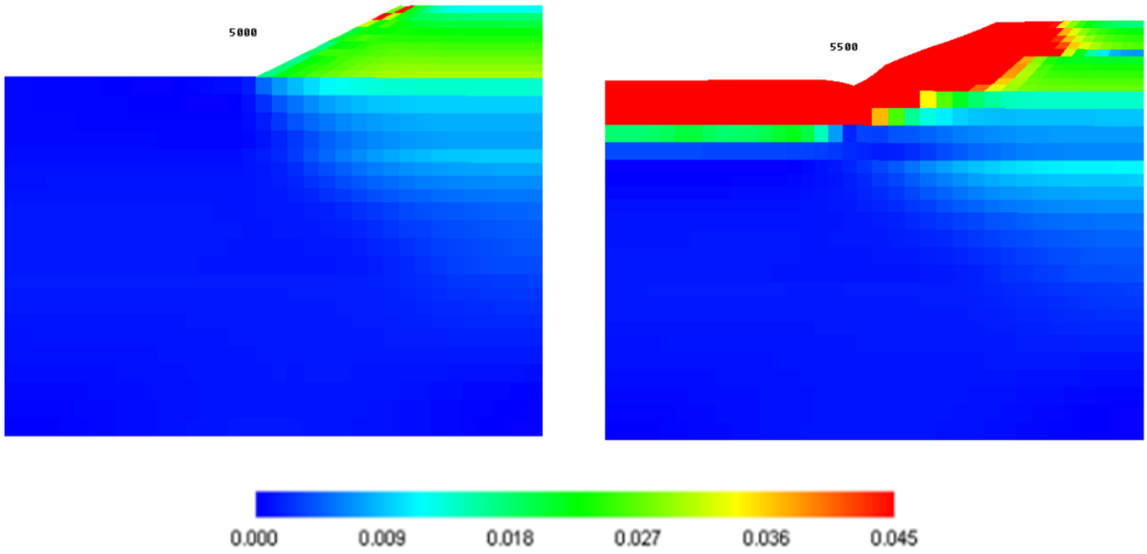

(a) after 463 days (b) after 509 days

Figure 4.18: Distribution of shear strain with time for case no. 4

4.5.3 Pore Water Pressure (Case 4)

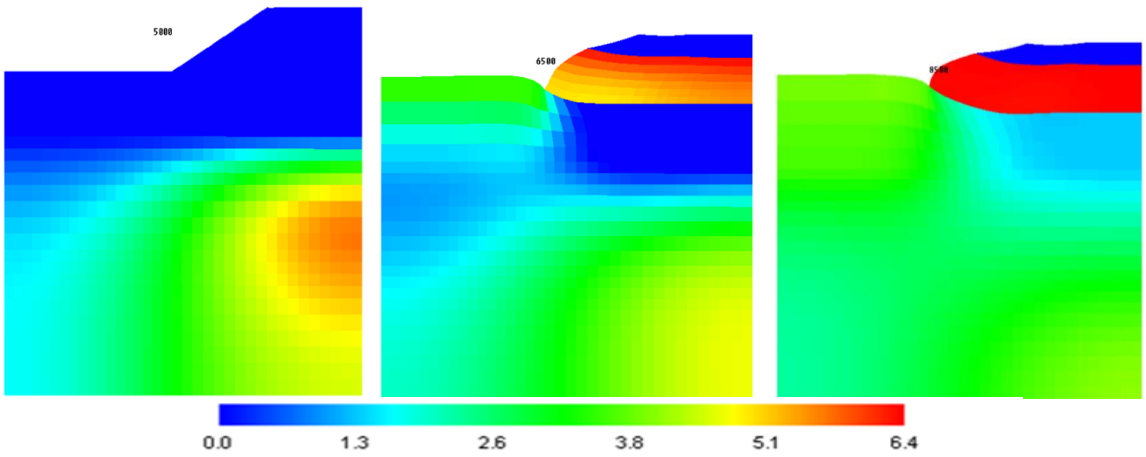

(a) after 463 days (b) after 602 days (c) after 740 days

Figure 4.19: Distribution of pore water pressure with time (case 4): unit (tf/m^2).

Figure 4.19 shows the distribution of pore water pressure for case 4 with respect to time. Before the failure of the slope there was very little pore water pressure below the embankment and almost zero pore water pressure in the first layer of the base and the embankment. As the water level rises some amount of pore water pressure develops at the bottom portion of the embankment which is almost 5.1 tf/m^2. At the time of failure there is the maximum amount of pore water pressure at bottom portion of the embankment and its value is about 6.4 tf/m^2. From the results it is clear that the pore water pressure is minimized by significant amount for case no. 4 compared to all the other cases before.

4.5.4 Displacement Vector (Case4)

Increasing the slopes horizontal component has significantly increased the stabilization of the slope compared to case 1 and case 2. In figure 4.20 vertical displacement vector shows the that the direction of the vertical displacement of the soil particles is very much lowered than the previous cases. This time the maximum displacement vector is 1 cm which is the minimum displacement vector in all the four cases.

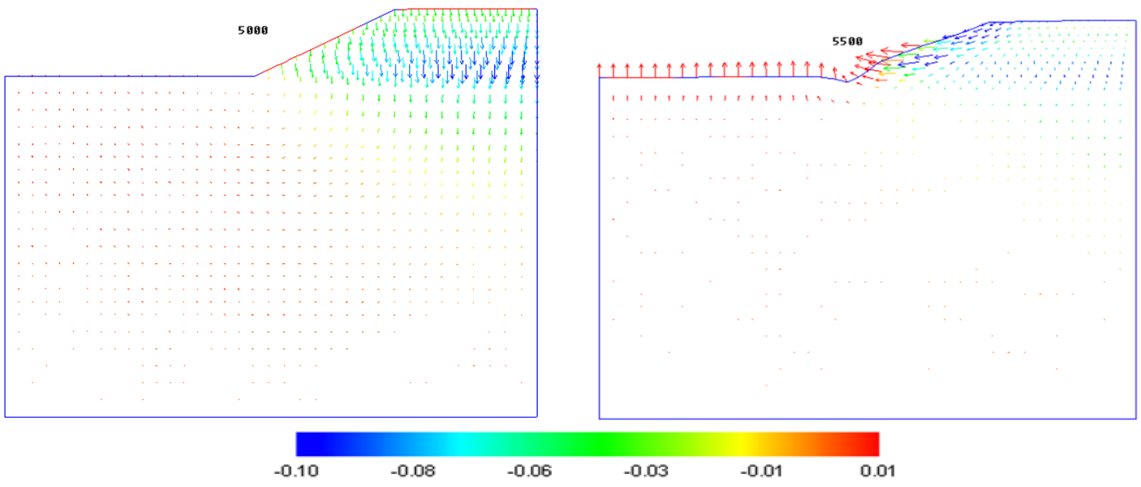

(a) after 463 days (b) after 509 days

Figure 4.20: Displacement vector with time for Case 4 (unit: meter)

4.5.5 Surface Settlement (Case 4)

For case 4 the total length of base is taken as 30m. Figure 4.20 represents the plot for the surface settlement of the base with respect to time. There is a maximum settlement of 7.4 cm after 2 years which is the greatest settlement in all the four cases. As the settlement is greater so the stabilization of the embankment is greater. Some amount of negative settlement or upward thrust is seen at the left side of base surface. So it makes clear that increasing the slopes horizontal component make the slope more stable.

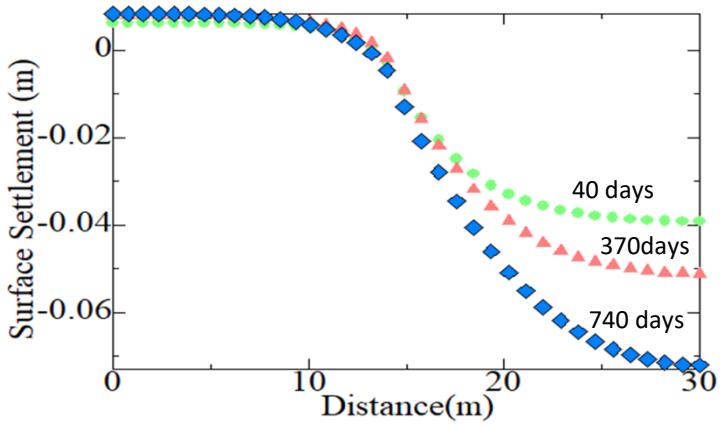

Figure 4.21: Plot for surface settlement at different stages (case 4).

Chapter 5 Conclusion

5.1 General

Natural slope instability is a major concern in the area where failures might cause catastrophic destruction on the surrounding area. The failures might be triggered by internal or external factors that cause imbalance to natural forces. An internal triggering factor is the factor that causes failure due to internal changes, such as increasing pore water pressure and or imbalanced forces developed due to external load.

The analyses performed in this study given the specific conditions of soil properties, slope geometry, and pattern of water-level changes showed that the water-level fluctuations resulted in lowering of stability and development of vertical deformations at the slope crest. The stability decrease is to assign to the fact that the groundwater table is increasing for each water level fluctuation. Though, since rapid changes of pore pressures and flow rates were noticed within the slope, other upcoming issues could probably occur as well suddenly as in the long term. The development of the pore-pressure peak values shows how the pore pressure at the end of each water level fluctuation, slowly becomes more and more large. If such fluctuations are taking place for a long time, increased pore pressures could falsely remain high. If then the fluctuation stops, the water levels would go back to equilibrium, and the extra shear strength would be lost.

Despite the fact that the absolute magnitudes of differences identified in this study were sufficient vertical displacement, pore water pressures, shear strain etc. these do nonetheless demonstrate important dissimilarities concerning the ability to capture/simulate real soil-water interactions and changes.

The results obtained in this study are reflecting effects occurred under the specified conditions of hydraulic conductivity, rate of water-level change, and slope geometry.
Since these factors are unquestionably affecting processes taking place within a watercourse slope, it would be reasonable to include variation also of such non constitutive

parameters in further studies. Results from this study indicate that the highway sections we considered are critical places from a slope stability point of view.

5.2 To be further considered

Future research using the results getting from different stability analyses will focus on the following areas as this study did not address them:

- Stability analysis for different slopes considering frequent water level rise
- Determination of allowable water level for stable slope
- Factor of safety will be determined.
- Required ground reinforcement strategy will be applied for slope protection.

References

- P. A. Lane and D. V. Griffiths, "Assessment of Stability of Slopes under Drawdown Conditions," J. Geotech.
- J. M. A. Johansson and T. Edeskär, "Effects of External Water-Level Fluctuations on Slope Stability," Electron. J.Geotech. Eng., vol. 19, no. K, pp. 2437–2463, 2014.
- Geoenvironmental Eng., vol. 126, no. 5, pp. 443–450, May 2000.
- Shahjahan M., (2010), "Materials Considered For Pavement and Embankment Design." MPhil Thesis, University of Birmingham, UK.
- Ameen, S.F. (1985); "Geotechnical Characteristics of Dhaka Clay" MSc. Engineering Thesis; Department of Civil Engineering, Bangladesh University of Engineering and Technology, Dhaka, Bangladesh.
- Aminullah, S.A. (2004); "Geotechnical Characteristics of Alluvial deposits of Bangladesh" M.Sc. Engineering thesis, Department of Civil Engineering, Bangladesh University of Engineering & Technology, Dhaka, Bangladesh.
- Bhattachariyya, S.K. (2009), "Design of Embankment for Bangladesh." *MPhil Thesis,* University of Birmingham, UK.
- Skempton, A.W. and Bjerrum, L., (1957) "A contribution to the settlement analysis of foundation on clay." Geotechnique, 7:168 – 178.
- Bishop, A. (1955). The Use of the Slip Circle in the Stability Analysis of Slope. Geotechnique, Vol. 5 (No. 1), pp. 7-17.
- Bishop, A. (1955). The Use of the Slip Circle in the Stability Analysis of Slope. *Geotechnique, Vol. 5* (No. 1), pp. 7-17.
- Fellenius, W. (1936). Calculation of Stability of Earth Dams. *Transactions, 2nd Congress Large Dams, Vol. 4,* p. 445. Washington D.C. New York: John Wiley and Sons Inc.
- Lambe, T. and Whitmen, R. (1969). *Soil Mechanics.* New York: John Wiley and Sons Inc.
- Mitchell R.A and Mitchell J.K. (1992). Stability Evaluation of Waste Landfills. *Stability and Performance of Slope and Embankments-II* (pp. 1152-1187). Berkeley, CA: 31 American Societies of Civil Engineers.

- Morgenstern, N., & Price, V. (1965). The Analysis of the Stability of General Slip Surfaces. *Geotechnique, Vol. 15* (No. 1), pp. 77-93.
- Lee W., Thomas S., Sunil S., and Glenn M.. 2002. *Slope Stability and Stabilization Methods.* 2nd Edition . New York : John Wiley & Sons, (2002). ISBN 0-471-38493-3.
- *Chowdury, R.N. (1978). Slope Analysis. Amsterdam : Elsevier Scientific Publishing Company, 1978. ISBN 0-444-41662-5.*
- Nakai, T. and Hinokio M. 2004. A simple elastoplastic model for normally and over consolidated soils with unified material parameters, Soils and Foundations, 44(2): 53-70.
- Nakai, T., Shahin, H. M., Kikumoto, M., Kyokawa, H., Zhang, F., Farias, M. M. 2011. A simple and unified three-dimensional model to describe various characteristics of soils, Soils and Foundations, 51(6): 1149-1168.

APPENDIX

REVIEW OF THE EXTENDED SUBLOADING t_{ij} MODEL

This model, despite the use of a small number of material parameters, can describe properly the following typical features of soil behaviors (Nakai and Hinokio, 2004 & Nakai et al., 2011):

(i) Influence of intermediate principal stress on the deformation and strength of geomaterials.

(ii) Dependence of the direction of plastic flow on the stress paths.

(iii) Influence of density and/or confining pressure on the deformation and strength of geomaterials.

(iv) The behavior of structured soils such as naturally deposited soils.

A brief description of the above mentioned features of this model can be made as follows:

Influence of intermediate principal stress is considered by defining yield function f with modified stress t_{ij} (i.e., defining the yield function with the stress invariants (t_N and t_S) instead of (p and q) and considering associate flow rule in t_{ij} –space instead of σ_{ij} –space (Nakai and Mihara (1984)). The stress and strain increment tensors and their parameters using ordinary concept and t_{ij}-concept are compared in Table 2. As shown in Fig. 6, the stress tensors and parameters in the ordinary models are defined as the quantities related to normal and parallel components of σ_{ij} to the octahedral plane. On the other hand, as shown in Fig. 7, the stress tensors and stress parameters of the t_{ij}-concept are those of normal and parallel components of the modified stress t_{ij} to the spatially mobilized plane (briefly SMP; Matsuoka and Nakai (1974)).

Figure 8(a) shows the yield surfaces of an elastoplastic model based on the t_{ij} concept, represented on the $t_N - t_S$ plane, in which the direction of plastic values are assigned as the direction cosines of the Specially Mobilized Plane according to the following equation (Nakai (1989)).

$$a_i = \sqrt{\frac{I_3}{I_2 \sigma_i}} \quad (i = 1,2,3) \qquad (1)$$

where σ_i (i=1,2,3) are the three principal stresses, I_2, and I_3 are the second and third invariants of σ_{ij}, The principal axes of t_{ij} coincide with those of σ_{ij}, because the principal axes of a_{ij} and σ_{ij} are identical.

According to subloading surface concept, yield surface (subloading surface) has not only to expand but also to shrink for the present stress state to lie always on the surface, and the yield function is written as a function of the mean stress t_N and stress ratio $X \equiv t_S / t_N$ based on t_{ij} by Eq.(2).

$$F = H \text{ or } f = F - H = 0 \qquad (2)$$

Where, $F = (\lambda - \kappa) \ln \frac{t_{N1}}{t_{N0}} = (\lambda - \kappa) \left\{ \ln \frac{t_N}{t_{N0}} + \varsigma(X) \right\}$ and $H = \left(-\Delta e\right)^p = (1 + e_0) \cdot \varepsilon_v^p$

Here, t_{N1} determines the size of the yield surface (the value of t_N at X=0), t_{N0} is the value of t_N at reference state. The symbols λ and κ denote compression index and swelling index, respectively, and e_0 is the void ratio at reference state. $\varsigma(X)$ is an increasing function of stress ratio $X(=t_S/t_N)$ which satisfies the condition $\varsigma(0)=0$. In this research, the expression for $\varsigma(X)$ is assumed as,

$$\varsigma\left(X\right) = \frac{1}{\beta}\left(\frac{X}{\mathrm{M}^*}\right)^{\beta} \quad (\square : \text{material parameter}) \quad (3)$$

The value of M* in Eq.(3) is expressed as follows using principal stress ratio $X_{CS} \equiv (t_S/t_N)_{CS}$ and plastic strain increment ratio $Y_{CS} \equiv (d\varepsilon_{SMP}^{*p} / d\gamma_{SMP}^{*p})_{CS}$ at critical state:

$$\mathrm{M}^* = \left(X_{CS} + X_{CS}^{\beta - 1} Y_{CS} \right)^{1/\beta} \qquad (4)$$

and these ratios X_{CS} and Y_{CS} are represented by the principal stress ratio at critical state in triaxial compression R_{CS}:

$$X_{CS} = \frac{\sqrt{2}}{3}\left(\sqrt{R_{CS}} - \frac{1}{\sqrt{R_{CS}}}\right) \quad (5)$$

$$Y_{CS} = \frac{1-\sqrt{R_{CS}}}{\sqrt{2}\left(\sqrt{R_{CS}}+0.5\right)} \quad (6)$$

In elastoplastic theory, total strain increment consists of elastic and plastic strain increments as

$$d\varepsilon_{ij} = d\varepsilon_{ij}^{e} + d\varepsilon_{ij}^{p} \quad (7)$$

Here, plastic strain increment is divided into component $d\varepsilon_{ij}^{p(AF)}$, which satisfies associate flow rule in the space of modified stress t_{ij}, and isotropic compression component $d\varepsilon_{ij}^{p(IC)}$as given in Eq.(8).

$$d\varepsilon_{ij}^{p} = d\varepsilon_{ij}^{p(AF)} + d\varepsilon_{ij}^{p(IC)} \quad (8)$$

The components of strain increment are expressed as,

$$d\varepsilon_{ij}^{p(AF)} = \Lambda \frac{\partial F}{\partial t_{ij}} \quad (9)$$

$$d\varepsilon_{ij}^{p(IC)} = \Lambda^{(IC)} \frac{\delta_{ij}}{3} \quad (10)$$

Here, Λ is the proportionality constant, δ_{ij} is Kronecker's delta. Dividing plastic strain increment into two components as in Eqs.(8) to (10), for the same yield function, this model can take into consideration feature (ii), i.e., the dependence of the direction of plastic flow on the stress paths.

Referring to the subloading surface concept by Hashiguchi (1980) and revising it, i.e., adding the term $G(\rho)$ in the denominator of the proportionality constant Λ of normal

consolidated condition, influence of density is considered. In the modeling based on the subloading surface concept (Hashiguchi, 1980), it is assumed that the current stress point always passes over the yield surface (subloading surface) whether plastic deformation occurs or not. The proportionality constant Λ is expressed as

$$\Lambda = \frac{\dfrac{\partial F}{\partial \sigma_{ij}} d\sigma_{ij} - \dfrac{\lambda - \kappa}{t_{N1}} \langle dt_N \rangle}{(1+e_0)\left(\dfrac{\partial F}{\partial t_{kk}} + \dfrac{G(\rho)}{t_N} \right)} = \left(\frac{\dfrac{\partial F}{\partial \sigma_{ij}} D^e_{ijkl} d\varepsilon_{kl}}{h_p + \dfrac{\partial F}{\partial \sigma_{mn}} D^e_{mnop} \dfrac{\partial F}{\partial t_{op}}} \right) \quad (11)$$

and

$$\Lambda^{(IC)} = \frac{\dfrac{\lambda - \kappa}{t_{N1}} \langle dt_N \rangle}{(1+e_0)\left(1 + \dfrac{G(\rho)}{(\lambda - \kappa) a_{kk}} \right)} \quad (12)$$

Here, the symbol < > denotes Macauley bracket.

As shown in Figure 8(b), the initial and current void ratios for over consolidated soils are expressed as e_0 and e and the state variable □□which represents the influence of density is defined as □=e_N-e and its initial value is (□□=e_{N0}-e_0). In the definition of Λ as in Eq.(11), ρ decreases with the development of plastic deformation and eventually becomes zero. To satisfy this condition, $G(\rho)$ should be a increasing function of ρ which satisfies $G(0) = 0$, such as

$G(\rho) = sign(\rho) a \rho^2$ (a: material parameter) (13)

The evolution rule of ρ is given as

$$d\rho = -(1+e_0) \frac{G(\rho)}{t_N} \Lambda \quad (14)$$

In feature (iv), the stress-strain behavior of structured soil can be described by considering not only the effect of density described above but also the effect of bonding. Two state

variables ρ related to density and ω representing the bonding effect are used to consider feature (iv). Here, the evolution rule of □ is then given as

$$d\rho = -(1+e_0)\left\{\frac{G(\rho)}{t_N} + \frac{Q(\omega)}{t_N}\right\}\Lambda \qquad (15)$$

The evolution rule of ω is given as

$$d\omega = -(1+e_0)\frac{Q(\omega)}{t_N}\Lambda \qquad (16)$$

In the present model, the following linear increasing function $Q(\omega)$ is adopted:

$$Q(\omega) = b\omega \qquad (17)$$

Finally, the proportionality constant Λ is expressed as:

$$\Lambda = \frac{\frac{\partial F}{\partial \sigma_{ij}} d\sigma_{ij}}{(1+e_0)\left(\frac{\partial F}{\partial t_{kk}} + \frac{G(\rho)}{t_N} + \frac{Q(\omega)}{t_N}\right)} = \frac{dF}{h^p} \qquad (18)$$

The loading condition of soil through its hardening process to softening process is presented as follows:

$$\begin{cases} d\varepsilon_{ij}^p \neq 0 & if \quad \Lambda = \dfrac{dF}{h^p} \geq 0 \\ d\varepsilon_{ij}^p = 0 & otherwise \end{cases} \qquad (19)$$